*MRI*

MRI was performed with a 3T MRI unit using a 32-channel array coil to obtain a high signal-to-noise ratio [6]. Heavily T2-weighted 3D constructive interference in the steady-state imaging was obtained for anatomic reference and 3D-FLAIR was then performed to detect perilymph enhancement while suppressing the signal from the endolymph. The details of the MRI protocol were described previously [4,7,8]. All images were attached to the electronic medical record and reviewed by a radiologist who was blinded to the patient's medical history.

The contrasting effects of cochlear fluid were evaluated semiquantitatively. A region of interest (ROI) was set manually in the basal turn of the cochlea on the 3D-FLAIR image. The signal intensity ratio (SIR) was defined as the signal intensity of the basal turn divided by that of a circular ROI in the cerebellar hemisphere. An example of ROI setting is shown in Figure 1. The averaged SIR value was measured three times and designated as the SIR for each ear. The SIR values were compared between the precontrast images and between the affected ear and the unaffected ear.

Grading of endolymphatic hydrops was evaluated in the vestibule and cochlea according to the criteria described previously [9].

## Results

The clinical findings in 10 patients with sudden deafness are summarized in Table I. The patients were five men and five women whose mean age (± SD) was 58.8 (± 12.0) years. MRI revealed an asymptomatic left dural arteriovenous fistula in patient no. 5. Patient no. 9 had experienced left sudden deafness 8 months after she experienced right

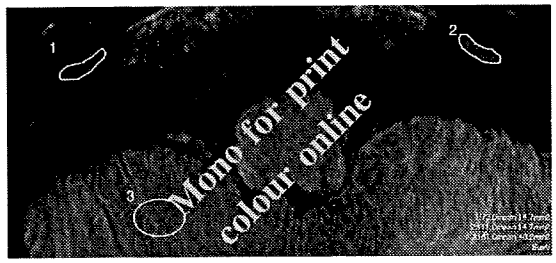


Figure 1. An example of the region of interest (ROI) setting on a contrast-enhanced 3D-FLAIR image. The ROI for the cochlear fluid signal intensity measurement was drawn manually around the basal turn of the cochlea. The circular ROI for the signal intensity measurement of the cerebellum was set in the most artifact-free area of the ipsilateral cerebellum. The signal intensity ratio was calculated as the value shown in the lower right of the figure.

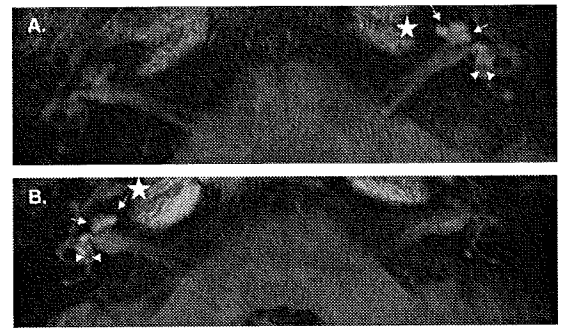


Figure 2. 3D-FLAIR MRI after intravenous Gd injection. (a) A 72-year-old man with left sudden deafness (patient no. 6). (b) A 67-year-old man with right sudden deafness (patient no. 10). Gd enhancement was obtained in both ears, and the affected ear (asterisks) showed bright signals compared with the unaffected ear. Arrows indicate the cochlea and arrowheads indicate the endolymphatic spaces in the vestibule.

sudden deafness. Four patients (nos 4, 6, 7, and 10) experienced vertigo in addition to hearing loss. The average interval between the onset of hearing loss and undergoing MRI was 10.3 ± 5.2 days. Hearing recovery was complete in three patients, marked in one patient, slight in two patients, and unchanged in four patients despite intravenous and/or intratympanic steroid therapy.

Precontrast MRI was performed in four patients and the SIR between the cochlea and cerebellum varied from 0.36 to 1.11 (0.55 ± 0.08). The SIR at contrast varied from 0.45 to 2.17 (1.05 ± 0.50) in 11 affected ears and from 0.43 to 1.48 (0.78 ± 0.29) in nine unaffected ears. In five of nine patients with unilateral sudden deafness, a difference in the contrasting effect (affected ear vs unaffected ear) could be obtained. 3D-FLAIR MRI showed low signals of the endolymph surrounded by high signals of the perilymph. The Gd distribution was recognized in the vestibule and semicircular canals of 10 affected ears, in which no significant vestibular hydrops was observed. Meanwhile, it was recognized in the cochlea of five affected ears, in which no cochlear hydrops was observed. In the remaining vestibules and cochleas of affected ears, the Gd enhancement was too faint to evaluate the endolymphatic hydrops. Typical MRI images for patient nos 6 and 10 are shown in Figure 2; Gd distribution was sufficient to observe inner ear fluid spaces.

## Discussion

Intravenous Gd injection has three advantages in the evaluation of the inner ear. First, the affected ear can be compared with the unaffected ear; second, the

clinician can observe whether the blood–labyrinthine barrier is disrupted; and third, the Gd injection method is readily available.

We previously reported pre- and post-contrast high signals in the affected inner ear of patients with sudden deafness who were examined with 3D-FLAIR MRI [1,10]. Such high signals may reflect minor hemorrhage or an increased concentration of protein in the inner ear fluid and a disrupted blood–labyrinthine barrier. Our present study revealed that waiting 4 h after intravenous Gd injection and using a double dose of Gd increases the post-contrast signals.

The ratio between the signal intensity of the inner ear and that of the cerebellar hemisphere has been reported in healthy ears [2]: in four ears of two healthy volunteers, the SIR values were $0.22 \pm 0.12$ before the injection and $0.90 \pm 0.11$ at 4 h after the Gd injection of 0.1 mmol/kg. We found SIR values of $0.55 \pm 0.08$ in precontrast images of the unaffected ear. In the affected ears of five patients, contrasting effects were recognized and the SIR was higher than in healthy subjects. The SIR may be a good indicator for the semiquantitative evaluation of disruption of the blood–labyrinthine barrier. Semiquantitative expression of the signal intensity may be useful for comparing the results between patients or between ears. However, we acknowledge that the SIR was based on signals only at the basal turn of the cochlea in this study.

Because the blood–endolymph barrier is extremely tight compared with the blood–perilymph barrier, Gd administered intravenously enters the perilymph but does not enter the endolymph [11]. This difference makes it possible to visualize the endolymphatic spaces of the inner ear using 3D-FLAIR MRI after intravenous Gd injection. The present study showed a distinction between the endolymph and perilymph in the vestibule on MRI after intravenous Gd injection in patients with sudden deafness. One limitation of this study relates to the distinction between the endolymphatic and perilymphatic images. Although the endolymphatic spaces of the vestibule were recognized in 10 affected ears, we could acquire images of the enhanced structure of the cochlea only in 5 affected ears. It was more difficult to observe the contrast in the cochlea than in the vestibule, possibly because the endolymphatic space volume is smaller in the cochlea than in the vestibule. In a 3D computerized model made from specimens of the temporal bone, the average of the cochlear endolymphatic volume was calculated to be one-fifth that of the vestibular endolymphatic volume in normal ears [12]. The endolymphatic space may be visualized more easily in patients with endolymphatic hydrops in the cochlea [13].

At present, even with advanced technology, we cannot achieve constant visualization of all of the cochlear endolymphatic space after intravenous Gd administration. However, increasing the permeability of the blood vessels in the blood–labyrinthine barrier by the intravenous injection of Gd enhances the perilymphatic spaces, allowing recognition of the endolymphatic spaces, which are not enhanced. To increase the precision of the diagnosis, additional technological development and improvement of the contrasting effect are needed. It is also important to clarify the relationships between the MRI findings and clinical manifestations. Further studies with a large number of subjects are warranted to investigate the disease further.

## Conclusion

This is the first report to demonstrate the distinction between the endolymph and perilymph on MRI after intravenous Gd injection in patients with sudden deafness. The ratio between the signal intensities of the inner ear and the cerebellar hemisphere may be a good indicator for evaluating the disruption of the blood–labyrinthine barrier in sudden deafness. This study protocol has potential as a method for the fine detection of the pathology of various inner ear diseases.

## Acknowledgments

This study was supported by research grants from the Ministry of Health, Labour and Welfare in Japan. The authors report no conflicts of interest. The authors alone are responsible for the content and writing of the paper.

## References

[1] Yoshida T, Sugiura M, Naganawa S, Teranishi M, Nakata S, Nakashima T. Three-dimensional fluid-attenuated inversion recovery magnetic resonance imaging findings and prognosis in sudden sensorineural hearing loss. Laryngoscope 2008;118:1433–7.

[2] Naganawa S, Komada T, Fukatsu H, Ishigaki T, Takizawa O. Observation of contrast enhancement in the cochlear fluid space of healthy subject using a 3D-FLAIR sequence at 3 Tesla. Eur Radiol 2006;16:733–7.

[3] Carfrae MJ, Holtzman A, Eames F, Parnes SM, Lupinetti A. 3 Tesla delayed contrast magnetic resonance imaging evaluation of Ménière's disease. Laryngoscope 2008;118:501–5.

[4] Nakashima T, Naganawa S, Sugiura M, Teranishi M, Sone M, Hayashi H, et al Visualization of endolymphatic hydrops in patients with Ménière's disease. Laryngoscope 2007;117:415–20.

[5] Nakashima T, Kuno K, Yanagita N. Evaluation of prostaglandin E1 therapy for sudden deafness. Laryngoscope 1989;99:542–6.

[6] Naganawa S, Nakashima T. Cutting edge of inner ear MRI. Acta Otolaryngol Suppl 2009;560:15–21.

[7] Naganawa S, Satake H, Kawamura M, Fukatsu H, Sone M, Nakashima T. Separate visualization of endolymphatic space, perilymphatic space and bone by a single pulse sequence; 3D-inversion recovery imaging utilizing real reconstruction after intratympanic Gd-DTPA administration at 3 Tesla. Eur Radiol 2008;18:920–4.

[8] Naganawa S, Sugiura M, Kawamura M, Fukatsu H, Sone M, Nakashima T. Imaging of endolymphatic and perilymphatic fluid at 3T after intratympanic administration of gadolinium-diethylenetriamine pentaacetic acid. AJNR Am J Neuroradiol 2008;29:724–6.

[9] Nakashima T, Naganawa S, Pyykkö I, Gibson WPR, Sone M, Nakata S, et al Grading of endolymphatic hydrops using magnetic resonance imaging. Acta Otolaryngol Suppl 2009;560:5–8.

[10] Sugiura M, Naganawa S, Teranishi M, Nakashima T. Three-dimensional fluid-attenuated inversion recovery magnetic resonance imaging findings in patients with sudden sensorineural hearing loss. Laryngoscope 2006;116: 1451–4.

[11] Zou J, Poe D, Bjelke B, Pyykkö I. Visualization of inner ear disorders with MRI in vivo: from animal models to human application. Acta Otolaryngol Suppl 2009;560:22–31.

[12] Teranishi M, Yoshida T, Katayama N, Hayashi H, Otake H, Nakata S, et al 3D computerized model of endolymphatic hydrops from specimens of temporal bone. Acta Otolaryngol Suppl 2009;560:43–7.

[13] Nakashima T, Naganawa S, Teranishi M, Tagaya M, Nakata S, Sone M, et al Endolymphatic hydrops revealed by intravenous gadolinium injection in patients with Ménière's disease. Acta Otolaryngol 2009 Aug 14, 1–6 (Epub ahead of print).

Original Paper

Audiology & Neurotology

Audiol Neurotol 2010;15:254–260
DOI: 10.1159/000258681

Received: January 9, 2009
Accepted after revision: September 24, 2009
Published online: November 17, 2009

# Relationship between the Degree of Endolymphatic Hydrops and Electrocochleography

Masako Yamamoto[a] Masaaki Teranishi[a] Shinji Naganawa[b] Hironao Otake[a] Makoto Sugiura[a, d] Tomoyuki Iwata[a] Tadao Yoshida[a] Naomi Katayama[a, c] Seiichi Nakata[a] Michihiko Sone[a] Tsutomu Nakashima[a]

Departments of [a]Otorhinolaryngology and [b]Radiology, Nagoya University Graduate School of Medicine, [c]Department of Nutrition and Food Science, Nagoya Women's University, Nagoya, and [d]Department of Otorhinolaryngology, Kariya Toyota General Hospital, Kariya, Japan

**Key Words**
Cochlear hydrops · Electrocochleography · Intratympanic gadolinium administration · Ménière's disease

**Abstract**
The purpose of this study was to evaluate the relationship between the endolymphatic space image obtained using magnetic resonance imaging (MRI) and the results of electrocochleography. Electrocochleography recordings were obtained from 25 ears of 24 patients, who underwent MRI 1 day after the intratympanic injection of gadolinium diethylenetriamine pentaacetic acid bismethylamide. The average summating potential to action potential (SP/AP) ratio in patients with significant endolymphatic hydrops in the cochlea was 54 ± 17%. However, in some patients who had significant endolymphatic hydrops in the cochlea, the SP/AP ratio was not enlarged. This may imply that elevation of the SP/AP ratio is related to not only the degree of endolymphatic hydrops but also to the persistence of hydrops.



## Introduction

Functional tests such as electrocochleography (EcochG), the glycerol test, and vestibular-evoked myogenic potential have been used to estimate endolymphatic hydrops [Conlon and Gibson, 2000; Klockhoff and Lindblom, 1966; Lin et al., 2006]. However, the exact relationship between the results of these functional tests and endolymphatic volume has not been clarified.

We have recently reported that endolymphatic hydrops can be visualized on 3-tesla magnetic resonance imaging (MRI) after intratympanic administration of gadolinium diethylenetriamine pentaacetic acid bismethylamide (Gd-DTPA-BMA) [Nakashima et al., 2007]. Although there remain aspects of the technique that require further confirmation through future studies including perhaps the use of a 7-tesla MRI scanner as these become more available, the use of 7-tesla MRI to humans has not been permitted by the Pharmaceutical Affairs Law in our country so far. The purpose of this study was to examine the relationship between the endolymphatic space image obtained by 3-tesla MRI and the results of EcochG.

KARGER
Fax +41 61 306 12 34
E-Mail karger@karger.ch
www.karger.com


1420–3030/10/0154–0254$26.00/0

Accessible online at:
www.karger.com/aud

Dr. Masako Yamamoto
Department of Otorhinolaryngology
Nagoya University Graduate School of Medicine
65, Tsurumai-cho, Showa-ku, Nagoya 466-8550 (Japan)
Tel. +81 52 744 2323, Fax +81 52 744 2325, E-Mail masakoy@med.nagoya-u.ac.jp

**Table 1.** Clinical manifestations, degree of endolymphatic hydrops, and EcochG

| Patient No. | Age; sex | Clinical diagnosis | Low-frequency hearing level, dB | Hearing level at 1000 Hz dB | High-frequency hearing level, dB | Time from onset of symptoms months | Disequilibrium | Degree of endolymphatic hydrops in the cochlea | Degree of endolymphatic hydrops in the vestibule | SP/AP % |
|---|---|---|---|---|---|---|---|---|---|---|
| 1 | 46; M | definite Ménière's | 67 | 60 | 60 | 103 | yes | significant | significant | 48 |
| 2 | 38; M | definite Ménière's | 30 | 40 | 112 | 5 | yes | mild | significant | 38 |
| 3 | 47; F | definite Ménière's | 20 | 25 | 33 | 6 | yes | mild | mild | 22 |
| 4 | 42; M | definite Ménière's | 42 | 30 | 55 | 30 | yes | significant | significant | 71 |
| 5 | 66; M | definite Ménière's | 35 | 45 | 50 | 80 | yes | significant | significant | 45 |
| 6 | 54; F | definite Ménière's | 37 | 35 | 50 | 1 | yes | significant | significant | 44 |
| 7 | 39; F | definite Ménière's | 25 | 10 | 10 | 11 | yes | none | none | 29 |
| 8 | 55; M | definite Ménière's | 42 | 5 | 37 | 15 | yes | significant | significant | 83 |
| 9 | 74; F | probable Ménière's | 90 | 60 | 68 | 2 | yes | significant | significant | 60 |
| 10 | 42; M | probable Ménière's | 47 | 60 | 75 | 79 | yes | significant | significant | 66 |
| 11 | 44; F | possible Ménière's | 13 | 10 | 10 | 1 | yes | none | none | 42 |
| | | | 13 | 5 | 13 | 1 | yes | none | none | 39 |
| 12 | 38; M | possible Ménière's | 15 | 10 | 5 | 25 | yes | none | none | 24 |
| 13 | 70; F | possible Ménière's | 63 | 55 | 38 | 124 | yes | none | mild | 52 |
| 14 | 44; F | possible Ménière's | 42 | 30 | 25 | 1 | yes | significant | significant | 41 |
| 15 | 69; F | possible Ménière's | 27 | 15 | 37 | 87 | yes | significant | significant | 60 |
| 16 | 51; M | possible Ménière's | 23 | 15 | 42 | 1 | yes | significant | significant | 31 |
| 17 | 26; F | possible Ménière's | 10 | 10 | 8 | 14 | yes | mild | significant | 34 |
| 18 | 38; M | DEH | 92 | 65 | 53 | 122 | yes | significant | significant | 77 |
| 19 | 66; M | DEH | 35 | 25 | 47 | 234 | no | mild | significant | 20 |
| 20 | 50; F | fluctuating HL | 27 | 10 | 22 | 2 | no | mild | none | 19 |
| 21 | 60; F | fluctuating HL | 38 | 10 | 13 | 48 | no | mild | mild | 36 |
| 22 | 66; F | fluctuating HL | 93 | 60 | 40 | 9 | no | significant | mild | 50 |
| 23 | 54; M | fluctuating HL | 30 | 20 | 37 | 3 | no | significant | significant | 30 |
| 24 | 44; F | fluctuating HL | 38 | 5 | 12 | 5 | no | mild | mild | 23 |

Patients No. 9 and 10 had one definitive episode of vertigo with hearing loss. In patient No. 11, who had episodic vertigo of the Ménière's type without hearing loss, Gd-DTPA-BMA was injected bilaterally. Patient No. 12 had episodic vertigo of the Ménière's type without hearing loss but with aural fullness on the left. Patients No. 13, 14, 15, and 16 had fluctuating hearing loss with disequilibrium but without definitive episodes. Patient No. 17 had episodic vertigo of the Ménière's type without hearing loss but with left tinnitus.

DEH = Delayed endolymphatic hydrops; fluctuating HL = fluctuating hearing loss without disequilibrium. Low-frequency hearing level: average of hearing level at 125, 250, and 500 Hz. High-frequency hearing level: average of hearing level at 2000, 4000, and 8000 Hz.

## Subjects and Methods

*Subjects*

The relationship between the endolymphatic space image and the results of EcochG was examined in 25 ears of 24 patients, whose mean age was 50.7 years (range, 26–74 years). Eleven patients were men and 13 were women; 8 had definite Ménière's disease, 2 had probable Ménière's disease, 7 had possible Ménière's disease, 2 had delayed endolymphatic hydrops, and 5 had fluctuating hearing loss without disequilibrium. The age, sex, side injected with Gd-DTPA-BMA (Omniscan, Daiichi-Sankyo Pharmaceutical Co. Ltd., Tokyo, Japan), presence or absence of disequilibrium, and the time from onset of symptoms in each patient are presented in table 1. The diagnosis of Ménière's disease was based on the 1995 American Academy of Otolaryngology-Head and Neck Surgery guidelines for the diagnosis of Ménière's disease [Committee on Hearing and Equilibrium, 1995]. The concept behind the diagnosis of delayed endolymphatic hydrops has been described in the literature [Schuknecht, 1978; Schuknecht et al., 1990]. The patients underwent MRI 1 day after the intratympanic injection of Gd-DTPA-BMA. The protocol of the study was approved by the Ethics Review Committee of the Nagoya University School of Medicine (approval numbers 369, 369-2, 369-3, 369-4). All patients gave their informed consent to the participation in this study. Their written informed consent was attached to the electronic medical record after the patient gave permission, in accordance with the suggestion of the Ethics Review Committee.

*Intratympanic Gadolinium Injection*

The detailed methods for intratympanic Gd-DTPA-BMA injection have been reported previously [Nakashima et al., 2007]. Gd-DTPA-BMA was diluted 8-fold with saline (v/v 1:7) or 16-fold

with saline (v/v 1:15). The patient was placed in the supine position with the head turned about 30° away from the sagittal line toward the other ear, and the diluted Gd-DTPA-BMA was injected intratympanically through the tympanic membrane using a 23-gauge needle and a 1-ml syringe. The amount of diluted Gd-DTPA-BMA injected was 0.3–0.5 ml. After the injection, the patient remained in the supine position for 60 min with the head turned about 60° away from the sagittal line toward the other ear.

*MRI Scans*

MRI scans were performed with a 3-tesla MR unit (Trio, Siemens, Erlangen, Germany) using a receive-only 12-channel phased array coil, as described previously [Naganawa et al., 2006; Sugiura et al., 2006]. $T_1$-weighted three-dimensional (3D) fast low-angle shot (FLASH), conventional 3D fluid-attenuated inversion recovery (FLAIR), and 3D inversion recovery turbo spin echo (IR TSE) with real reconstruction was performed. 3D FLAIR can differentiate the endolymphatic space from the perilymphatic space but not from the surrounding bone. 3D IR TSE with real reconstruction can visualize the endolymphatic space, perilymphatic space, and surrounding bone separately, as described previously [Naganawa et al., 2008a, b]. $T_2$-weighted imaging with 3D constructive interference in the steady state was performed to obtain reference images of the labyrinthine fluid space anatomy. The parameters for 3D FLASH were as follows: repetition time (TR) of 4.3 ms, echo time (TE) of 1.97 ms, flip angle of 10° with radio frequency spoiling, matrix size of 256 × 256, and 96 axial 0.8-mm-thick slices covering the posterior fossa with a 16-$cm^2$ field of view. The number of excitations was 2, giving a total scan time of 2 min 51 s. The parameters for imaging with 3D constructive interference in the steady state were as follows: TR of 11.42 ms, TE of 5.71 ms, flip angle of 50°, matrix size of 320 × 320, and 48 axial 0.8-mm-thick slices with a 16-$cm^2$ field of view. The number of excitations was 1, and the scan time was 3 min 42 s. The parameters for 3D FLAIR and 3D IR TSE were as follows: TR of 9000 ms, TE of 134 ms, inversion time of 2500 ms for 3D FLAIR and inversion time of 1700 ms for 3D IR TSE, flip angle of 180° (constant) for the TSE refocusing echo train, echo train length of 23, matrix size of 384 × 384, and 12 axial 2-mm-thick slices covering the labyrinth with a 16-$cm^2$ field of view, acquired using the GRAPPA parallel imaging technique with an acceleration factor of 2 [Griswold et al., 2002]. The number of excitations was 1, and the scan time was 14 min [Naganawa et al., 2008a].

*Image Evaluation of the Endolymphatic Space*

The degree of endolymphatic hydrops in the cochlea and in the vestibule was classified as none, mild, or significant, according to the criteria described previously [Nakashima et al., 2009], by a radiologist who did not know the clinical progress of the patients. In the cochlea, patients classified as having no hydrops show no displacement of Reissner's membrane; those with mild hydrops show displacement of Reissner's membrane but the area of the endolymphatic space does not exceed the area of the scala vestibuli, and in those with significant hydrops the area of the endolymphatic space exceeds the area of the scala vestibuli. In the vestibule, the grading was determined by the ratio of the area of the endolymphatic space to the vestibular fluid space (sum of the endolymphatic and perilymphatic spaces). Patients with no hydrops have a ratio of one third or less, those with mild hydrops have between one third and a half, and those with significant hydrops have a ratio of more than a half.

*Audiometry*

Hearing levels were evaluated using an audiometer (Model AA-61BN or AA-79S, Rion, Tokyo, Japan) in a sound-attenuated room. If the patient did not respond to the maximum sound level produced by the audiometer, we defined the threshold as 5 dB added to the maximum level.

*Electrocochleography*

A silver ball electrode was placed on the posteroinferior quadrant of the external ear canal, close to the tympanic membrane. Before the electrode was placed, the skin of the electrode area was cleaned with skin preparation gel for bioelectrical measurements (Skin Pure, Nihon Koden, Tokyo, Japan), and then electrode paste (Biotach, GE Yokogawa Medical, Tokyo, Japan) was spread over the skin area. EcochG was performed with the patient lying down in a sound-attenuated room. The reference electrode was close to the earlobe, and the ground electrode was on the forehead. The click stimuli were presented 4 times a second with rarefaction and condensation polarity (Synax 2100, NEC Medical Systems, Tokyo, Japan). The signal was added 500 times through the band-pass filter (100–3000 Hz). The summating potential to action potential (SP/AP) ratio was calculated when SP and AP were clear [Nakashima et al., 2007].

*Statistical Analyses*

Statistical analyses were performed by using SPSS. The data were analyzed using the Kruskal-Wallis test, Mann-Whitney U test, Pearson's correlation coefficient test, and Spearman's rank correlation coefficient test. Pearson's correlation coefficient test was selected to compare the SP/AP ratio and hearing levels, while Spearman's rank correlation coefficient test was selected to compare the SP/AP ratio and the time from onset of symptoms in patients who had significant endolymphatic hydrops, because the values in the former comparison distributed normally and those in the latter did not distribute normally. Significance was set at $p < 0.05$.

## Results

The degree of endolymphatic hydrops, the SP/AP ratio, the average hearing levels of low-tone (125, 250, and 500 Hz) and high-tone frequencies (2000, 4000, and 8000 Hz), and the hearing level at 1000 Hz in each patient are presented in table 1. Examples of cases of endolymphatic hydrops in the cochlea and in the vestibule are shown in figures 1 and 2, respectively. Endolymphatic space was recognized as areas with low signal intensity partly surrounded by high signal intensity perilymphatic fluid on 3D FLAIR. 3D FLAIR can differentiate the endolymphatic space from the perilymphatic space, but not from the surrounding bone. 3D IR with real reconstruction can separate the signals of the perilymphatic space (positive

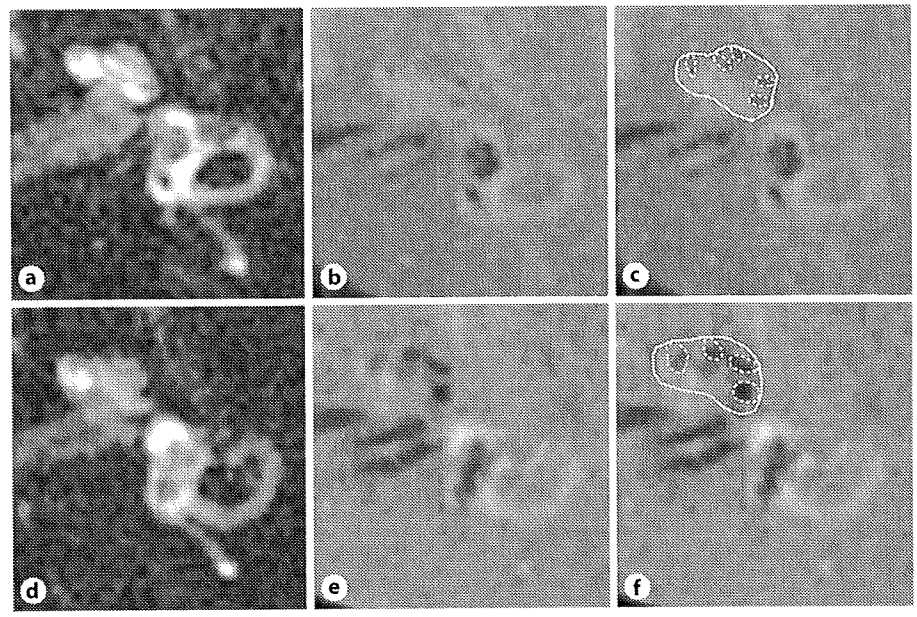


**Fig. 1.** MRI showing endolymphatic hydrops in the cochlea. **a**, **d** 3D FLAIR MRI. **b**, **e** 3D IR MRI with real reconstruction. **c**, **f** Line drawing figures of **b** and **e**. The dotted lines indicate endolymphatic spaces of cochlea turns. The solid line indicates fluid area of the cochlea. **a–c** Images showing mild endolymphatic hydrops in the cochlea of patient No. 3 in table 1. **d–f** Images showing significant endolymphatic hydrops in the cochlea of patient No. 6 in table 1.

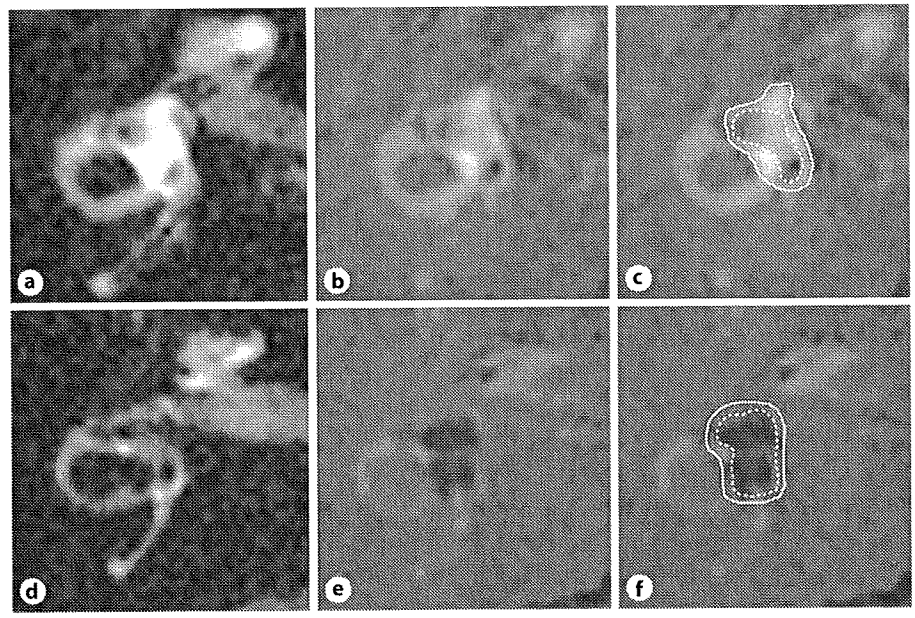


**Fig. 2.** MRI showing endolymphatic hydrops in the vestibule. **a**, **d** 3D FLAIR MRI. **b**, **e** 3D IR MRI with real reconstruction. **c**, **f** Line drawing figures of **b** and **e**. **a–c** Images showing mild endolymphatic hydrops in the vestibule of patient No. 13 in table 1. In **c**, the area of endolymphatic space (dotted circle) to total fluid space (solid line) in the vestibule is 42.2%. **d–f** Images showing significant endolymphatic hydrops in the vestibule of patient No. 4 in table 1. In **f**, the area of endolymphatic space (dotted circle) to total fluid space (solid line) in the vestibule is 61.4%.

value), endolymphatic space (negative value), and bone (near zero). The low signal area of the surrounding bone on 3D FLAIR showed a near-zero signal on 3D IR with real reconstruction, as described previously [Naganawa et al., 2008a, b]. The average SP/AP ratio of all patients was 43 ± 18%. The average SP/AP ratio of patients with no, mild, and significant endolymphatic hydrops in the cochlea was 37 ± 11, 27 ± 8, and 54 ± 17%, respectively. The relationship between the degree of endolymphatic hydrops in the cochlea and the SP/AP ratio is shown in figure 3. A significant difference in the SP/AP ratio was found among the three groups (Kruskal-Wallis test, $p < 0.05$). A significant difference in the SP/AP ratio was found between no and significant endolymphatic hydrops, and mild and significant endolymphatic hydrops (Mann-Whitney U test, $p < 0.05$). However, no significant difference in the SP/AP ratio was found between no and mild endolymphatic hydrops.

The worse the average hearing levels of low-tone frequencies (125, 250, and 500 Hz) and high-tone frequen-

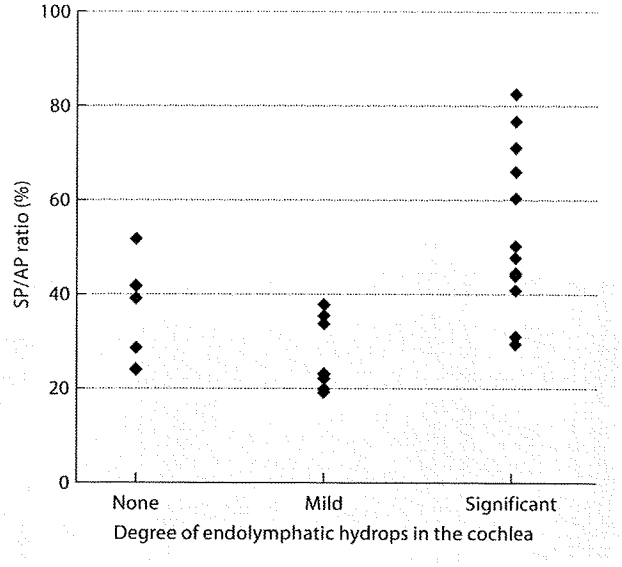


**Fig. 3.** Distribution of the SP/AP ratio according to the degree of endolymphatic hydrops in the cochlea. The SP/AP ratio in patients with significant endolymphatic hydrops in the cochlea was more elevated than the SP/AP ratio in patients with none and mild endolymphatic hydrops in the cochlea ($p < 0.05$).

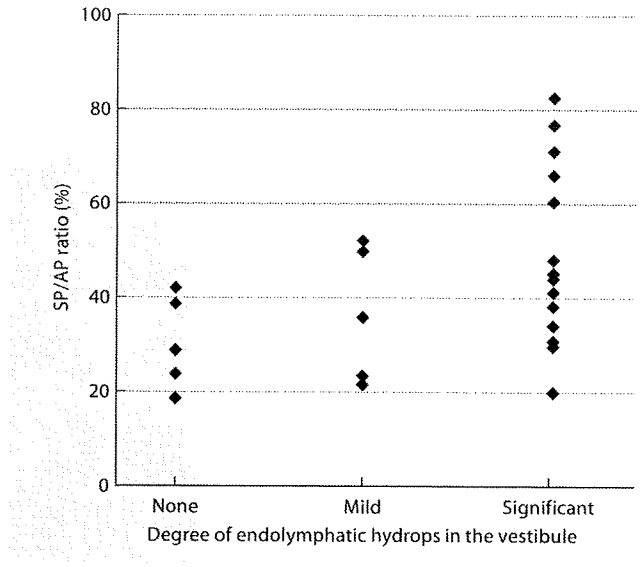


**Fig. 4.** Distribution of the SP/AP ratio according to the degree of endolymphatic hydrops in the vestibule. No significant difference of the SP/AP ratio was found among the three groups.

cies (2000, 4000, and 8000 Hz), the more the SP/AP ratio was enlarged. This correlation was also found in the hearing level of mid-tone frequency (1000 Hz) (Pearson's correlation, $p < 0.05$).

The relationship between the degree of endolymphatic hydrops in the vestibule and the SP/AP ratio is shown in figure 4. Although the SP/AP ratio tended to be enlarged in the group with significant endolymphatic hydrops in the vestibule compared to the groups with no and mild endolymphatic hydrops, no statistical significance was found among the three groups (Kruskal-Wallis test, $p > 0.05$).

Sex and the time from onset of symptoms were not significantly related to the SP/AP ratio. However, in patients who had significant endolymphatic hydrops in the cochlea, the time from onset of symptoms was significantly related to the SP/AP ratio. In patients who had significant endolymphatic hydrops in the cochlea, a longer time from onset of symptoms was associated with a greater enlargement of the SP/AP ratio (Spearman's rank correlation, $p < 0.05$) (fig. 5).

The SP/AP ratios in patients No. 16 and 23 were not enlarged, although the endolymphatic hydrops was sig-

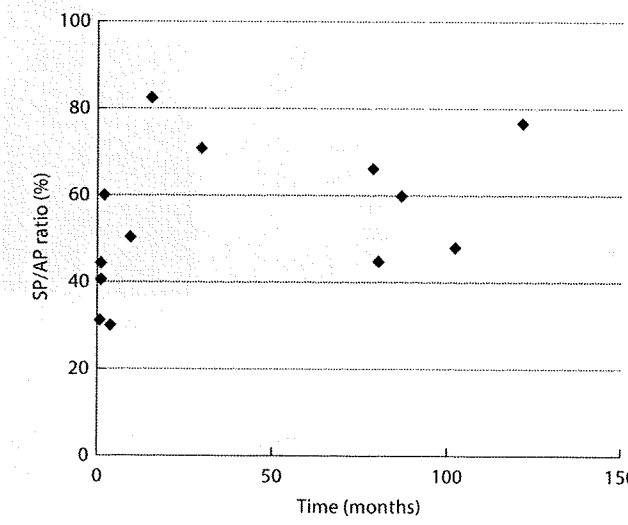


**Fig. 5.** The relationship between the SP/AP ratio in patients with significant endolymphatic hydrops in the cochlea and the time from onset of symptoms. Enlargement of the SP/AP ratio was associated with a longer time from onset of symptoms.

nificant. In patient No. 16, 1 month had elapsed between the onset of symptoms and having MRI and EcochG, and in patient No. 23, the interval was 3 months.

## Discussion

In this study, we performed extratympanic EcochG, of which clinical usefulness in the diagnosis of Ménière's disease was reported in past reports [Chung et al., 2004; Hwang et al., 2008; Pappas et al., 2000; Bonucci and Hyppolito, 2009]. Our results showed that the SP/AP ratio was enlarged in patients with significant endolymphatic hydrops except for 2 patients with a relatively short history of the disease. Ohashi et al. [1991] noted that a normal SP/AP ratio is frequently obtained in many patients in the early stage of Ménière's disease, who show slight hearing loss. They proposed that this reflects a stage of the disease in which the hair cell malfunction has not yet developed despite the presence of endolymphatic hydrops. Ge and Shea [2002] reported that an enlarged SP/AP ratio occurs more frequently in association with greater hearing loss and with a longer duration of the disease. Ferraro and Durrant [2006] reported a significant relationship between EcochG results and the symptoms displayed at the time of testing. Mori et al. [1993] reported a significant correlation between a negative summating potential abnormality and the high-frequency hearing level but not the low-frequency hearing level. Kitahara et al. [1981] reported that a worse hearing loss at 500–2000 Hz was found in ears with an abnormal SP/AP ratio than in ears with a normal SP/AP ratio. These previous reports and our present findings from the endolymphatic images indicate that an enlarged SP/AP ratio does not necessarily reflect endolymphatic hydrops. Progression of hearing loss or a long history of the disease may be necessary to elevate the SP/AP ratio.

MRI after intratympanic administration of Gd-DTPA-BMA and EcochG can be performed at almost the same time, and these examinations can be repeated to follow up the patients. Adding MRI after intratympanic administration of Gd-DTPA-BMA to one of the common examinations used to follow up patients will help clinicians understand more clearly the relationship between endolymphatic hydrops and EcochG.

## Conclusion

In our study of MRI taken after intratympanic Gd-DTPA-BMA administration, the SP/AP ratio was enlarged in patients with significant endolymphatic hydrops except for those examined within 3 months of onset of symptoms. The SP/AP ratio in patients with mild endolymphatic hydrops was not enlarged compared with the ratio in patients without endolymphatic hydrops. Diagnosis using MRI and functional tests enables one to understand inner ear diseases better.


## Acknowledgments

This study was supported by research grants from the Ministry of Education, Culture, Sports, Science and Technology, and the Ministry of Health, Labor and Welfare, Japan.


## References


Chung WH, Cho DY, Choi JY, Hong SH: Clinical usefulness of extratympanic electrocochleography in the diagnosis of Ménière's disease. Otol Neurotol 2004;25:144–149.

Conlon BJ, Gibson WPR: Electrocochleography in the diagnosis of Ménière's disease. Acta Otolaryngol 2000;120:480–483.

Committee on Hearing and Equilibrium: Committee on Hearing and Equilibrium guidelines for the diagnosis and evaluation of therapy in Ménière's disease. Otolaryngol Head Neck Surg 1995;113:181–185.

Ferraro JA, Durrant JD: Electrocochleography in the evaluation of patients with Ménière's disease/endolymphatic hydrops. J Am Acad Audiol 2006;17:45–68.

Ge X, Shea JJ Jr: Transtympanic electrocochleography: a 10-year experience. Otol Neurotol 2002;23:799–805.

Griswold MA, Jakob PM, Heidemann RM, Nittka M, Jellus V, Wang J, Kiefer B, Hasse A: Generalized autocalibrating partially parallel acquisitions (GRAPPA). Magn Reson Med 2002;47:1202–1210.

Hwang JH, Ho HC, Hsu CJ, Yang WS, Liu TC: Diagnostic value of combining bilateral electrocochleography results for unilateral Ménière's disease. Audiol Neurotol 2008;13:365–369.

Kitahara M, Takeda T, Yazawa Y, Matsubara H: Electrocochleography in the diagnosis of Ménière's disease; in Vosteen KH, Schuknecht H, Pfalz CR, et al (eds): Ménière's Disease. Pathogenesis, Diagnosis and Treatment. Stuttgart, Thieme, 1981, pp 163–169.

Klockhoff I, Lindblom U: Endolymphatic hydrops revealed by glycerol test. Preliminary report. Acta Otolaryngol 1966;61:459–462.

Lin MY, Timmer FC, Oriel BS, Zhou G, Guinan JJ, Kujawa SG, Herrmann BS, Merchant SN, Rauch SD: Vestibular evoked myogenic potentials (VEMP) can detect asymptomatic sacclar hydrops. Laryngoscope 2006;116:987–992.

Mori N, Asai H, Sakagami M: The role of summating potential in the diagnosis and management of Ménière's disease. Acta Otolaryngol Suppl 1993;501:51–53.

Naganawa S, Komada T, Fukatsu H, Ishigaki T, Takizawa O: Observation of contrast enhancement in the cochlear fluid space of healthy subjects using a 3D-FLAIR sequence at 3 Tesla. Eur Radiol 2006;16:733–737.

Naganawa S, Satake H, Iwano S, Fukatsu H, Sone M, Nakashima T: Imaging endolymphatic hydrops at 3 Tesla using 3D-FLAIR with intratympanic Gd-DTPA administration. Magn Reson Med Sci 2008a;7:85–91.

Naganawa S, Satake H, Kawamura M, Fukatsu H, Sone M, Nakashima T: Separate visualization of endolymphatic space, perilymphatic space and bone by a single pulse sequence: 3D-inversion recovery imaging utilizing real reconstruction after intratympanic Gd-DTPA administration at 3 Tesla. Eur Radiol 2008b;18:920–924.

Nakashima T, Naganawa S, Pyykkö I, Gibson WPR, Sone M, Nakata S, Teranishi M: Grading of endolymphatic hydrops using magnetic resonance imaging. Acta Otolaryngol Suppl 2009;129:5–8.

Nakashima T, Naganawa S, Sugiura M, Teranishi M, Sone M, Hayashi H, Nakata S, Katayama N, Ishida IM: Visualization of endolymphatic hydrops in patients with Ménière's disease. Laryngoscope 2007;117:415–420.

Ohashi T, Ochi K, Okada T, Takeyama I: Long-term follow-up of electrocochleogram in Ménière's disease. ORL J Otorhinolaryngol Relat Spec 1991;53:131–136.

Pappas DG Jr, Pappas DG Sr, Carmichael L, Hyatt DP, Toohey LM: Extratympanic electrocochleography: diagnostic and predictive value. Am J Otol 2000;21:81–87.

Schuknecht HF: Delayed endolymphatic hydrops. Ann Otol Rhinol Laryngol 1978;87:743–748.

Schuknecht HF, Suzuka Y, Zimmermann C: Delayed endolymphatic hydrops and its relationship to Ménière's disease. Ann Otol Rhinol Laryngol 1990;99:843–853.

Bonucci AS, Hyppolito MA: Comparison of the use of tympanic and extratympanic electrodes for electrocochleography. Laryngoscope 2009;119:563–566.

Sugiura M, Naganawa S, Teranishi M, Nakashima T: Three-dimensional fluid-attenuated inversion recovery magnetic resonance imaging findings in patients with sudden sensorineural hearing loss. Laryngoscope 2006;116:1451–1454.

Neuroradiology (2009) 51:855–863
DOI 10.1007/s00234-009-0588-6

HEAD AND NECK RADIOLOGY

# Increased signal intensity of the cochlea on pre- and post-contrast enhanced 3D-FLAIR in patients with vestibular schwannoma

**Masahiro Yamazaki · Shinji Naganawa · Hisashi Kawai · Takashi Nihashi · Hiroshi Fukatsu · Tsutomu Nakashima**

Received: 26 May 2009 / Accepted: 17 August 2009 / Published online: 29 August 2009


**Abstract**
*Introduction* In the vestibular schwannoma patients, the pathophysiologic mechanism of inner ear involvement is still unclear. We investigated the status of the cochleae in patients with vestibular schwannoma by evaluating the signal intensity of cochlear fluid on pre- and post-contrast enhanced thin section three-dimensional fluid-attenuated inversion recovery (3D-FLAIR).
*Methods* Twenty-eight patients were retrospectively analyzed. Post-contrast images were obtained in 18 patients, and 20 patients had the records of their pure-tone audiometry. Regions of interest of both cochleae (C) and of the medulla oblongata (M) were determined on 3D-FLAIR images by referring to 3D heavily T2-weighted images on a workstation. The signal intensity ratio between C and M on the 3D-FLAIR images (CM ratio) was then evaluated. In addition, correlation between the CM ratio and the hearing level was also evaluated.
*Results* The CM ratio of the affected side was significantly higher than that of the unaffected side ($p<0.001$). In the affected side, post-contrast signal elevation was observed ($p<0.005$). In 13 patients (26 cochleae) who underwent both gadolinium injection and the pure-tone audiometry, the post-contrast CM ratio correlated with hearing level ($p<0.05$).
*Conclusion* The results of the present study suggest that alteration of cochlear fluid composition and increased permeability of the blood–labyrinthine barrier exist in the affected side in patients with vestibular schwannoma. Furthermore, although weak, positive correlation between post-contrast cochlear signal intensity on 3D-FLAIR and hearing level warrants further study to clarify the relationship between 3D-FLAIR findings and prognosis of hearing preservation surgery.

**Keywords** Magnetic resonance · FLAIR · High resolution · Vestibular schwannoma · Cochlea

M. Yamazaki (✉) · S. Naganawa · H. Kawai · T. Nihashi
Department of Radiology, Graduate School of Medicine,
Nagoya University,
65 Tsurumai-cho, Showa-ku,
Nagoya 466-8550, Japan
e-mail: yamazaki@med.nagoya-u.ac.jp

H. Fukatsu
Department of Medical Informatics,
Aichi Medical University Hospital,
Nagakute, Japan

T. Nakashima
Department of Otorhinolaryngology,
Graduate School of Medicine, Nagoya University,
Nagoya, Japan

## Introduction

In patients with vestibular schwannoma, presenting complaints are unilateral hearing reduction or an episode of sudden hearing loss, although the pathophysiologic mechanism of inner ear involvement is still unclear. In past reports, Silverstein et al. suggested protein level elevation of cochlear perilymph in patients with vestibular schwannoma who underwent the labyrinthine tap as the diagnostic test [1–4]. However, the labyrinthine tap has since been completely abandoned due to the risk of causing deafness. Currently, CT or MR imaging is the differential diagnosis tools of choice in patients with hearing loss. Therefore, investigation into cochlear protein levels has necessarily been suspended for the time being.

CT is indicated to assess conduction hearing deficit, while MR is the procedure of choice for sensorineural hearing loss. Fluid-attenuated inversion recovery (FLAIR) imaging is sensitive in detecting high protein contents in fluids such as cerebrospinal fluid and various cystic intracranial mass lesions [5,6]. Three-dimensional FLAIR (3D-FLAIR) images can minimize the undesired inflow ghosts of cerebrospinal fluid flow [7] and enable recognition of the subtle compositional changes in lymph fluid in the inner ear that cannot be detected by T1-weighted images [8–10]. Furthermore, increased permeability of the blood–labyrinthine barrier can also be observed on post-contrast 3D-FLAIR images; this technique has been reported to be useful for pathophysiologic analysis of the inner ear in many auditory diseases, such as sudden sensorineural hearing loss (SNHL), cholesteatoma, and cochlear otosclerosis [11–13].

The purposes of the present study were to evaluate the signal intensity of cochlear fluid on pre- and post-contrast-enhanced thin sections by 3D-FLAIR in patients with vestibular schwannoma and to investigate the relationship between auditory function and signal alteration.

## Materials and methods

### Study population

This study was approved by the Ethics Review Committee of our institution (approval number 729). The requirement for informed patient consent was waived owing to the retrospective nature of the study. The records of 28 patients (ten male and 18 female; mean age, 62 years; range, 12–79 years) with unilateral vestibular schwannoma who underwent MR imaging of the inner ear, including 3D-FLAIR sequence, at our hospital from January 2007 to June 2008 were retrospectively examined. All of the patients had been diagnosed on the basis of typical MR imaging appearances by an experienced neuroradiologist (S. N.). In this patient group, there was no bilateral case, neurofibromatosis type 2, or intracochlear lesion. Two patients underwent surgical treatment, and one patient received gamma knife radiosurgery after diagnosis. The remaining 25 patients were followed without aggressive medical treatments, such as surgical treatment and gamma knife radiosurgery. Three patients had a history of gamma knife radiosurgery before coming to our hospital. Eighteen patients also had pre- and post-contrast MR imaging of the inner ear by intravenous administration of gadolinium-diethylenetriamine pentaacetic acid (Gd-DTPA; Magnevist, Bayer Yakuhin, Ltd., Osaka, Japan) or gadolinium-diethylenetriamine pentaacetic acid-bis (methylamide) (Gd-DTPA-BMA; Omniscan, Daiichi Sankyo Co., Ltd., Tokyo, Japan). Twenty patients had the records of their pure-tone audiometry data within a month of the MR examination. In other eight patients, it was impossible to obtain pure-tone audiometry data around the MR examination because some referred from other hospitals for MR imaging, and others had longer interval from pure-tone audiometry to the MR examination. Thirteen patients underwent both gadolinium injection and the pure-tone audiometry.

### MR imaging protocol

All patients underwent axial 3D-FLAIR, 3D-T1-weighted imaging (T1WI) and 3D heavily T2-weighted imaging (T2WI) of the inner ear. Images were obtained on whichever 3 T scanner (Magnetom Trio; Siemens AG, Erlangen, Germany) or on two types of 1.5 T scanners (Magnetom Avanto; Siemens AG, Erlangen, Germany or Excelart Vantage; Toshiba, Tokyo, Japan) using a receive-only, 12-channel (on Siemens Trio, Avanto) or 10-channel (on Toshiba Vantage), phased-array coil. Ten patients obtained MR imaging on Trio scanner, 12 patients on Avanto scanner, and six patients on Vantage scanner. Eighteen patients had 3D-FLAIR and 3D-T1WI after intravenous gadolinium contrast agent administration (Gd-DTPA or Gd-DTPA-BMA; 0.1 mmol/kg body weight in total amount). After the contrast was administered, 3D-T1WI was scanned first. Then, post-contrast 3D-FLAIR was initiated 7 min after the gadolinium was administered so that the contrast of 3D-FLAIR was determined approximately 10 min after the administration of gadolinium. The slice thickness of all images was 0.8 mm.

The sequence parameters for 3D-FLAIR, 3D-T1WI and 3D heavily T2WI are shown in Table 1. 3D-T1WI were obtained using a spoiled gradient echo sequence. 3D-heavily T2WI were obtained using a gradient echo-based sequence on a 3 T scanner and a spin echo-based sequence on 1.5 T scanners.

### MR imaging analysis

Image analysis was performed on a picture archiving and communication system workstation. In each patient, regions of interest (ROI) of both cochleae and of the medulla oblongata were determined on 3D-FLAIR images by referring to 3D heavily T2WI at a workstation (Fig. 1). The ROI were drawn around each cochlea on the 3D heavily T2WI at the level of the modiolus. Similarly, a ROI was drawn around the medulla oblongata on 3D heavily T2WI. Then, they were copied onto identical slices of 3D-FLAIR images, which provided the ROIs for the 3D-FLAIR images. The ratio of cochlear signal intensity to that of the medulla oblongata (CM ratio) on the 3D-FLAIR

**Table 1** MR sequence parameters.

| | Scanner | | |
|---|---|---|---|
| | 3T (Siemens Trio) | 1.5T (Siemens Avanto) | 1.5T (Toshiba Vantage) |
| 3D-FLAIR sequence parameters | | | |
| Repetition time (ms) | 9,000 | 8,000 | 9,000 |
| Echo time (ms) | 458 or 638 | 295 or 316 or 339 | 80 |
| Inversion time (ms) | 2,500 | 2,300 | 2,500 |
| Reconstructed voxel size ($mm^3$) | 0.7×0.7×0.8 | 0.8×0.8×0.8 | 0.7×0.7×0.8 |
| Echo train length | 119 or 171 | 141 | 68 |
| Echo space (ms) | 3.7 | 4.3 or 4.6 | 6.5 or 10 |
| Parallel factor | 2 [a] | 2 [a] | 2 [b] |
| Pulse sequence | SPACE | SPACE | FASE |
| Scan time (minutes' seconds") | 5' 26" | 6' 26" | 6' 45" |
| 3D-T1 weighted imaging sequence parameters | | | |
| Repetition time (ms) | 6.9 or 7.7 | 8.4 or 9.3 or 9.7 | 23.0 |
| Echo time (ms) | 3.3 | 3.5 or 3.6 or 3.9 or 4.4 or 4.6 | 5.5 |
| Reconstructed voxel size ($mm^3$) | 0.6×0.6×0.8 | 0.8×0.6×0.8 | 0.7×0.7×0.8 or 0.8×0.7×0.8 or 0.8×0.8×0.8 |
| Parallel factor | 2[a] | 2[a] | 1 |
| Pulse sequence | VIBE | VIBE | SPGR |
| Scan time (minutes' seconds") | 3' 49" or 4' 16" | 3' 31" or 3' 52" or 4' 02" | 3' 47" |
| 3D-heavily T2 weighted imaging sequence parameters | | | |
| Repetition time (ms) | 6.4 or 8.8 | 1,200 | 4,000 |
| Echo time (ms) | 3.2 or 4.4 | 262 or 264 | 240 or 300 |
| Reconstructed voxel size ($mm^3$) | 0.5×0.5×0.8 | 0.8×0.6×0.8 | 0.6×0.3×0.8 or 0.6×0.4×0.8 |
| Echo train length | – | 71 | 72 |
| Echo space (ms) | – | 5.7 or 6.1 | 15 |
| Parallel factor | 2[a] | 2[a] | 1 |
| Pulse sequence | CISS | SPACE | FASE |
| Scan time (minutes' seconds") | 3' 15" or 5' 13" | 4' 21" | 5' 56" |

[a] *GRAPPA* Generalized autocalibrating partially parallel acquisition

[b] SPEEDER A kind of SENSE (sensitivity encoding)

*SPACE* sampling perfection with application optimized contrast using different flip angle evolutions, *FASE* fast asymmetric spin echo, *VIBE* volumetric interpolated breath hold examination, *SPGR* spoiled gradient recalled acquisition in the steady state, *CISS* constructive interference in the steady state

images was determined for each cochlea. In a manner similar to 3D-FLAIR imaging, the CM ratio on 3D-T1WI was determined. The CM ratio was calculated in both pre-contrast and in post-contrast 3D-FLAIR and 3D-T1WI. The reason for selecting the medulla oblongata as the reference for calculating the CM ratio was to compare the cochlear signal intensity of affected side with that of unaffected side statistically. Tumors were classified into two groups, based on the presence or absence of extension to the cochlear area at the fundus of the internal auditory canal (IAC). The maximal linear diameters of the tumors were also measured on 3D heavily T2WI. These measurements were performed by one radiologist (M.Y.) who did have prior knowledge of the existence of vestibular schwannoma. Measuring the signal in a blinded manner was not feasible in this study.

## Audiological assessment

Hearing levels were evaluated using an audiometer (model AA-79S; Rion, Tokyo, Japan) in a sound-insulated chamber. If the patient did not respond to the maximum sound level produced by the audiometer, we defined the threshold as 5 dB added to the maximum level. The average hearing level was calculated as the mean of the hearing levels measured at 500, 1,000, 2,000, and 3,000 Hz on the basis of the American Academy of Otolaryngology—Head and Neck Surgery guidelines in vestibular schwannoma [14].

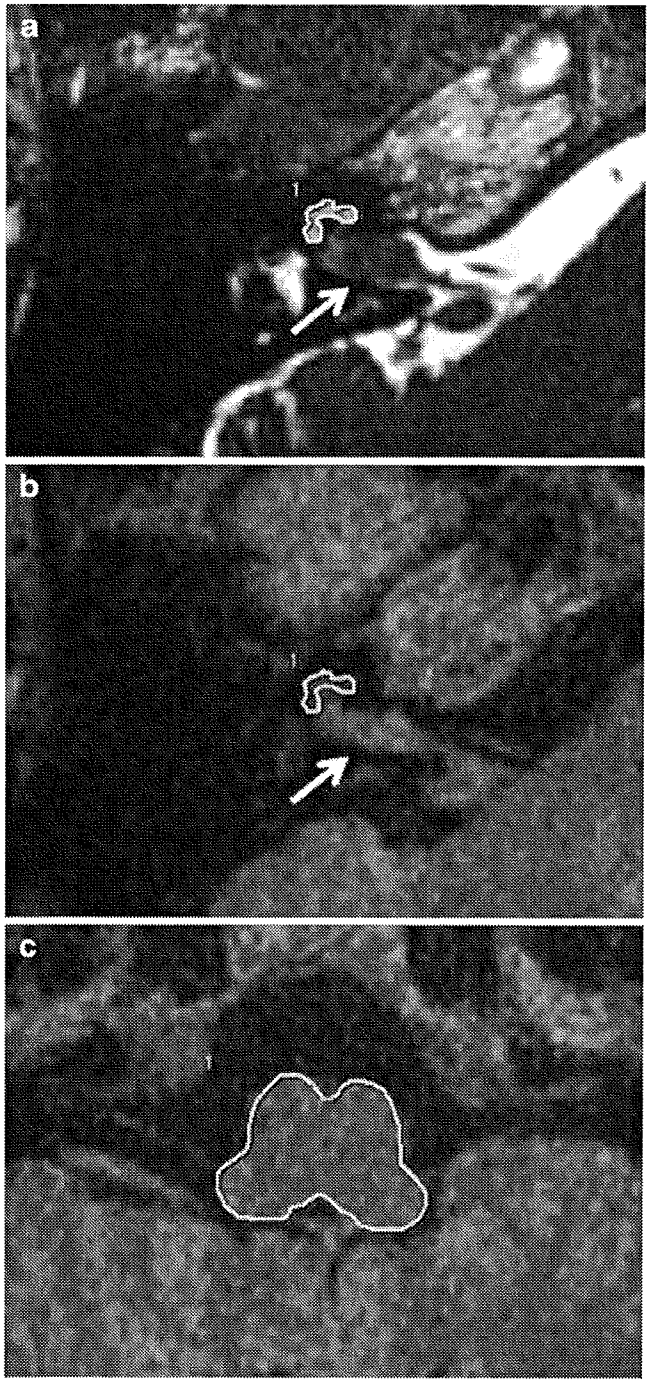


**Fig. 1** A 3D-CISS image and a 3D-FLAIR image at the level of the modiolus (**a**, **b**) and a 3D-FLAIR image at the level of the medulla oblongata (**c**) of a 36-year-old man with vestibular schwannoma in his right internal auditory canal (IAC) are presented. Vestibular schwannoma was detected in the IAC (*arrows* on **a**, **b**). The ROI of the cochlea were determined on 3D-FLAIR images by referring to 3D heavily T2WI at a workstation. The ROI were drawn around each cochlea on the 3D heavily T2WI at the level of the modiolus (**a**), then they were copied onto identical slices of 3D-FLAIR images (**b**), which provided the ROIs for 3D-FLAIR imaging. The ROIs of the medulla oblongata on 3D-FLAIR images were similarly set (**c**)

### Statistical analysis

Differences in CM ratio between the affected and unaffected sides, between pre- and post-contrast, and the hearing level difference between affected and unaffected sides were compared using a paired *t* test. The differences in CM ratio between the affected and unaffected sides were assessed in both pre-contrast and in post-contrast 3D-FLAIR and 3D-T1WI. Student's *t* test was used to compare the CM ratio on pre-contrast 3D-FLAIR images on the affected side between the groups with or without invasion of the fundus of the IAC. Differences in CM ratio of the affected side between 3 and 1.5 T scanners on both 3D-FLAIR and 3D-T1WI were compared also using Student's *t* test. The relationship between the CM ratio on pre-contrast 3D-FLAIR and tumor diameter was investigated using Pearson's correlation coefficient test. The relationship between the CM ratio on both pre- and post-contrast 3D-FLAIR images and hearing level was investigated using Spearman's correlation coefficient by rank test. In our statistical analysis, a value of $p<0.05$ represented statistical significance.

## Results

Fourteen of the 28 tumors had extension to the cochlear area at the fundus of the IAC, while the other 14 did not. The mean size of the vestibular schwannomas was 10.0 mm (range, 2.8–21.5 mm).

None of the patients showed a visible abnormality of medulla oblongata on all images and high signal of cochlea that would have suggested hemorrhage on pre-contrast 3D-T1WI. There was no significant difference between the affected side and unaffected side CM ratio on pre-contrast 3D-T1WI (the mean CM ratio was 0.46±0.07 on affected side, 0.46±0.07 on unaffected side, $p=0.93$). The mean CM ratio on the pre-contrast 3D-FLAIR images for the affected side was 0.59±0.18 while that for the unaffected side was 0.33±0.10 ($p<0.001$, Fig. 2). There was no significant difference in CM ratio on pre-contrast 3D-FLAIR and 3D-T1WI on the affected side between 3 T scanner (the mean CM ratio was 0.68±0.12 on 3D-FLAIR and 0.44±0.06 on 3D-T1WI) and 1.5 T scanners (the mean CM ratio was 0.54±0.19 on 3D-FLAIR and 0.47±0.08 on 3D-T1WI; $p=0.06$ on 3D-FLAIR, $p=0.20$ on 3D-T1WI). In addition, there was no significant difference in CM ratio on pre-contrast 3D-FLAIR images of the affected side between tumors with extension to the cochlear area at the fundus of the IAC (the mean CM ratio was 0.63±0.13) and those without extension (the mean CM ratio was 0.55±0.22) ($p=0.28$). Furthermore, there was no significant correlation between tumor diameter and CM ratio on pre-contrast 3D-FLAIR images ($r=0.37$, $p=0.05$).

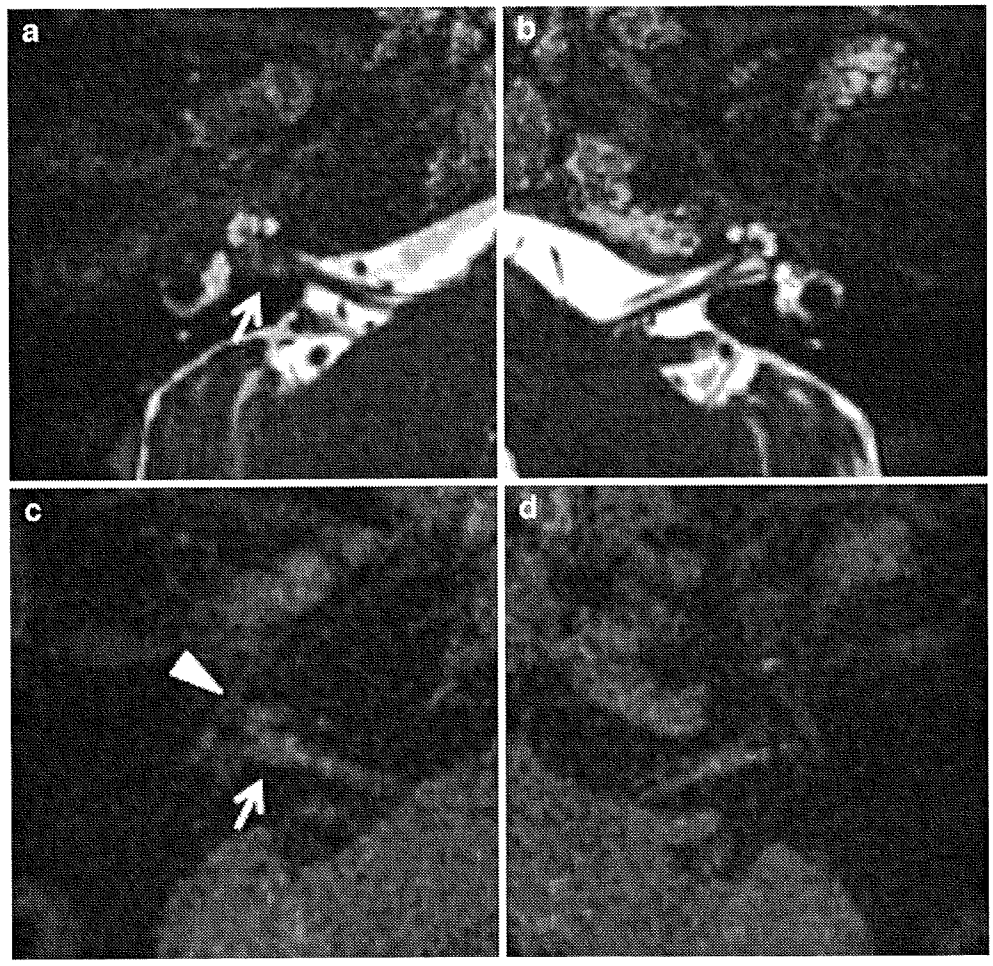


**Fig. 2** Bilateral 3D-CISS images (**a**, **b**) and pre-contrast 3D-FLAIR images (**c**, **d**) at the level of the modiolus of a 49-year-old man with vestibular schwannoma in his right internal auditory canal (*arrows* on **a**, **c**) are presented. A right cochlear signal intensity increase is seen on the 3D-FLAIR image (*arrowhead* on **c**). On the other hand, the left cochlear signal intensity on the 3D-FLAIR image is very faint, and it has ill-defined borders. On 3D-CISS images, cochlear signal intensity difference between both sides is not so obvious as 3D-FLAIR

In the 18 patients who had post-contrast imaging of the inner ear, the mean CM ratio on the post-contrast 3D-FLAIR images for the affected side was 0.74±0.15, while that for the unaffected side was 0.35±0.12 ($p<0.001$, Fig. 3). There was no significant difference between the affected and unaffected side CM ratio on post-contrast 3D-T1WI (the mean CM ratio was 0.46±0.08 on affected side, 0.44±0.07 on unaffected side, $p=0.26$). In the affected side of the 18 patients who had post-contrast imaging of the inner ear, the mean CM ratio on pre-contrast 3D-FLAIR images was 0.66±0.13, while that for the post-contrast images was 0.74±0.15 ($p<0.005$). There was no significant difference between pre- and post-contrast CM ratio on 3D-T1WI of the affected side (the mean CM ratio was 0.45±0.08 on pre-contrast, 0.45±0.07 on post-contrast, $p=0.60$). There was no significant difference in CM ratio on post-contrast 3D-FLAIR and 3D-T1WI on the affected side between 3 T scanner (the mean CM ratio was 0.80±0.13 on 3D-FLAIR and 0.45±0.07 on 3D-T1WI) and 1.5 T scanners (the mean CM ratio was 0.68±0.15 on 3D-FLAIR, 0.46±0.09 on 3D-T1WI; $p=0.09$ on 3D-FLAIR, $p=0.75$ on 3D-T1WI). In the unaffected side, there were no significant differences between pre- and post-contrast CM ratio on both 3D-FLAIR (the mean CM ratio was 0.33±0.11 on pre-contrast and 0.35±0.12 on post-contrast, $p=0.88$) and 3D-T1WI (the mean CM ratio was 0.46±0.07 on pre-contrast and 0.44±0.07 on post-contrast, $p=0.21$).

In the 20 patients who underwent a pure-tone audiometry, the mean hearing level for the affected side was 53.2±33.2 dB while that for the unaffected side was 22.7±14.3 dB ($p<0.001$). When we limit the evaluation only on affected side, Spearman's correlation coefficient by rank test showed no significant correlation between both pre- and post-contrast CM ratio on 3D-FLAIR images and hearing level (pre-contrast, $n=20$, $r=0.06$; post-contrast, $n=13$, $r=-0.02$). Meanwhile, provided that affected and unaffected side were assessed together, there was no significant correlation between pre-contrast CM ratio on 3D-FLAIR images and hearing level ($n=40$, $r=0.27$, $p=0.09$), although the CM ratio on post-contrast 3D-FLAIR images correlated with hearing level ($n=26$, $r=0.47$, $p<0.05$, Fig. 4).

## Discussion

The results of the present study suggest alteration of cochlear fluid composition in the affected side of patients

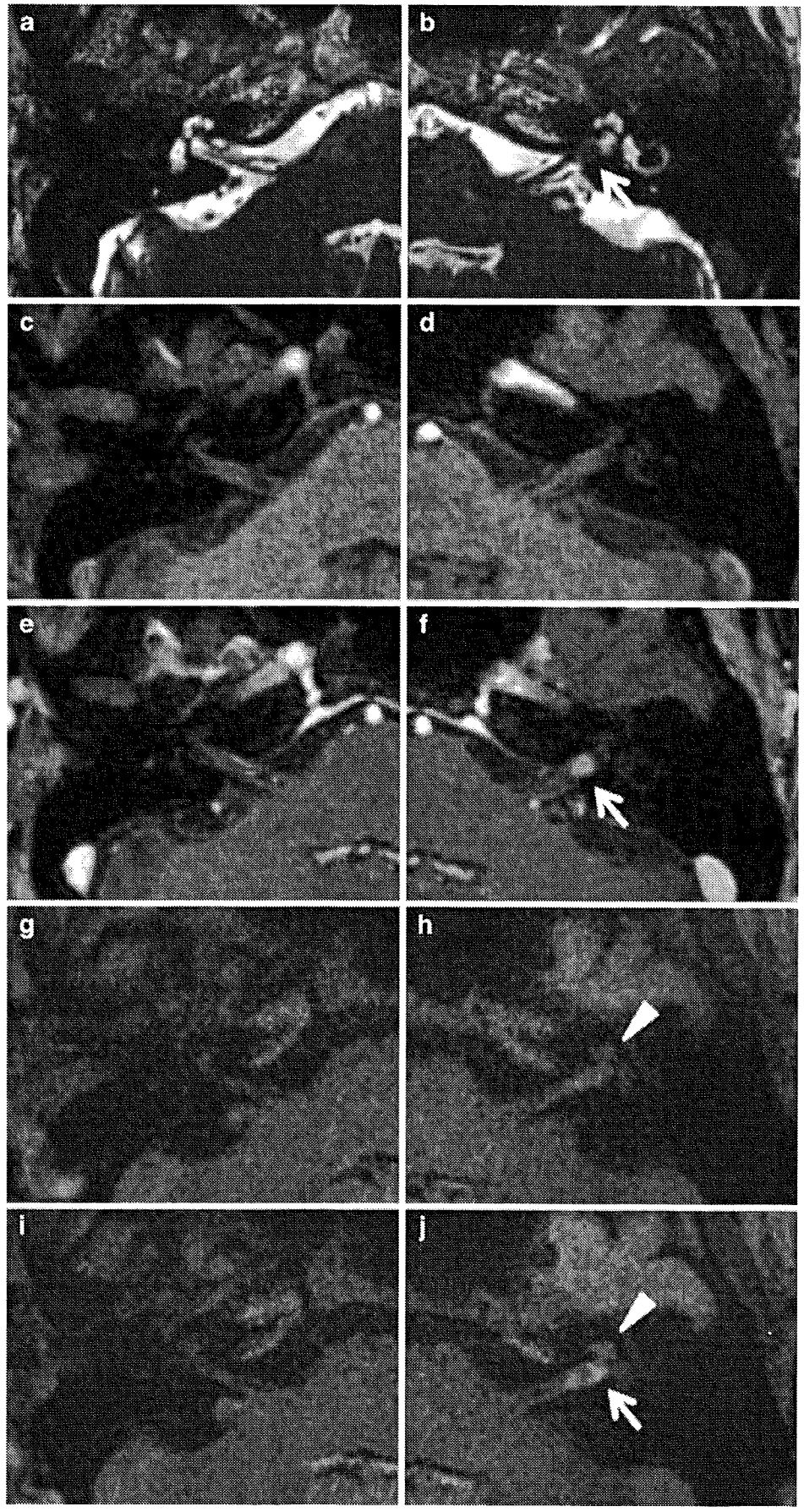


**Fig. 3** Bilateral 3D-CISS images (**a**, **b**), pre- (**c**, **d**), and post-contrast (**e**, **f**) 3D-T1WI, and pre- (**g**, **h**) and post-contrast (**i**, **j**) 3D-FLAIR images at the level of the modiolus of a 55-year-old woman with vestibular schwannoma in her left internal auditory canal (IAC, *arrow* on **b**, **f**) are presented. On the 3D-T1WI, there is no signal difference between both cochleae, and no signal elevation is observed after gadolinium injection. In contrast, on the pre-contrast 3D-FLAIR image, the left cochlear signal intensity increase is seen (*arrowhead* on **h**). On the post-contrast 3D-FLAIR image, further signal elevation of the left cochlea can be observed (*arrowhead* on **j**). In addition, leakage of gadolinium agent is seen at the fundus of the left IAC (*arrow* on **j**)

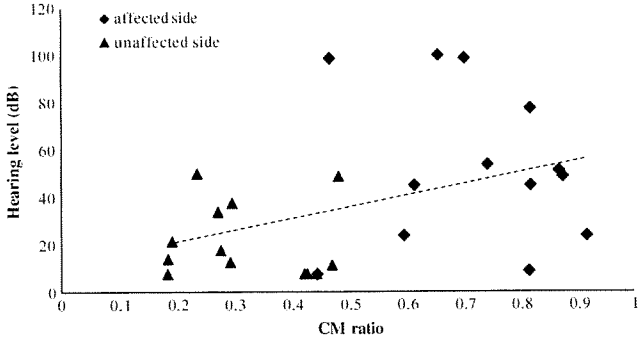


**Fig. 4** In all 13 patients (26 ears) who underwent both gadolinium injection and a pure-tone audiometry, the post-contrast CM ratio on 3D-FLAIR correlated with hearing level ($r$=0.47, $p$<0.05)

with vestibular schwannoma. This is consistent with previous studies using the surgical approach [1–4,15–17]. MR imaging using the 3D-FLAIR technique makes it possible to determine the condition of the inner ear lymph fluid without cerebrospinal fluid inflow and pulsation artifacts or invasive surgical procedures, which carry some risk of contamination of the perilymph with blood and other fluids. On 3D-T1WI, changes in inner ear lymph fluid composition cannot be recognized.

We also observed post-contrast signal elevation on the affected side. Usually, on 3D-FLAIR images, enhancement of the cochlear fluid cannot be detected at 10 min after gadolinium injection [18]. Therefore, this result suggests increased permeability of the blood–labyrinthine barrier in the affected side. On the other hand, there was no significant difference between pre- and post-contrast CM ratio on 3D-T1WI. The contrast effect on FLAIR is reported to be higher than T1WI at the concentration of extravasated gadolinium below 0.7 mmol/L [19,20]. It is more than probable that the leakage of gadolinium contrast agent to cochlear fluid is too low to be recognized on T1WI. Furthermore, provided that affected and unaffected side were assessed together, correlation between the post-contrast CM ratio on 3D-FLAIR images and the degree of hearing impairment was suggested, although no correlation was observed between the pre-contrast CM ratio and hearing level. Thus, it appears that, in patients with vestibular schwannoma, increased permeability of the blood–labyrinthine barrier in the cochlea may be one of the important causes of hearing loss, as seen in cases of meningitis, and noise-induced and sensorineural hearing loss [21–23]. However, when we evaluate only on the affected side, there was no significant correlation between CM ratio on 3D-FLAIR images and hearing level. This result is possibly caused by small number of patients; further accumulation of cases and additional evaluation are necessary. Additionally, although the correlation between tumor diameter and CM ratio on pre-contrast 3D-FLAIR images did not reach significance ($p$=0.05), the $r$ value of 0.37 obtained likely indicates that the reason for this result is the small number of patients included.

The protein level elevation of cochlear perilymph in patients with vestibular schwannoma was reported in past times, and the origin of the elevated protein was discussed in many studies [1–4,15–17,24–27]. There are three main hypotheses that explain the cause of increased cochlear perilymph protein level in patients with vestibular schwannoma. These are cochlear membrane damage by blood vessel stasis either in artery or vein resulting in increased permeability [2,16,24], neuroaxonal protein transport blockage in the cochlear nerve caused by tumor compression [17], and cell-mediated immune reaction in the inner ear to antigenic properties of vestibular schwannomas [26,27]. Each pattern could cause perilymph protein increase. However, a vascular disorder, more specifically increased permeability of the blood–labyrinthine barrier, might also be closely related to the degree of hearing loss in patients with vestibular schwannoma, based on the present study.

Yoshida et al. reported that cochlear signal intensity on 3D-FLAIR images in patients with SNHL was increased in many cases and that a high signal in the cochlea on pre-contrast 3D-FLAIR images is related to a poor hearing prognosis, although they found no relationship between cochlear signal intensity and initial hearing level [28]. Meanwhile, hearing improvement in patients who showed post-contrast enhancement on 3D-FLAIR images in the affected inner ear was not significantly different from that in patients who did not. Although the pathology of SNHL remains unclear, vascular compromise and immunologic diseases have been hypothesized [29,30], which might have something in common with the pathological hypotheses in vestibular schwannoma. Thus, pre-contrast cochlear signal intensity on 3D-FLAIR images might be a prognostic factor in patients with vestibular schwannoma. In addition, cochlear post-contrast 3D-FLAIR signal intensity has the potential for correlation with initial hearing level in patients with SNHL.

The 3D-FLAIR technique can provide high resolution images [31,32]. In addition, FLAIR images are sensitive in detecting a high protein content of fluid [5,6]. It is conceivable that a signal decrease on CISS images, which reflects liquid T2/T1 lowering, can indicate the existence of hemorrhage and/or a high protein content of fluid [33,34]. However, in past reports, most signal changes observed on 3D-FLAIR images could not be detected on CISS images [28,35,36]. Consequently, 3D-FLAIR images appear more sensitive in detecting a high protein content of fluid than CISS images. Furthermore, because signal changes in CISS images are represented as loss of intensity, it is difficult to completely avoid the influence of magnetic susceptibility artifacts and the partial volume effect [37]. Therefore, we applied 3D-FLAIR in the current investigation to evaluate

cochlear fluid composition changes in patients with vestibular schwannoma.

Somers et al. [34] reported that intra-labyrinthine signal intensity on CISS images should be a valuable tool for determining candidacy for hearing preservation surgery. When a cochlear signal intensity decrease is detected on CISS images, it is conceivable that a relatively strong composition change may arise in the lymph fluid. On the other hand, 3D-FLAIR images would be so sensitive in detecting the protein content of fluid that faint and reversible alterations in lymph fluid composition could be detected. Consequently, in the future, quantitative analysis of cochlear signal intensity using 3D-FLAIR images may be a prognostic indicator of hearing preservation surgery.

Recently, Bhadelia et al. [38] reported a cochlear FLAIR signal increase in patients with vestibular schwannoma using 5 mm section thickness, two-dimensional pre-contrast FLAIR imaging. They were able to place ROI within the cochlea without difficulty because the cochlea was markedly hyperintense on the affected side, although evaluation of the unaffected side and control subjects was difficult due to the small size of the cochlea. In our study, 0.8-mm-thick high-resolution isotropic 3D-FLAIR imaging was used, and the ROI were set with accuracy by referring to 3D heavily T2WI. On the other hand, our study has some limitations: Our retrospective study collected data from images taken by multiple MR scanners, group of patients was heterogeneous, and signal intensity measurement was semiquantitative without using external phantoms for reference.

In conclusion, the results of the present study suggest that alteration of cochlear fluid composition and increased permeability of the blood–labyrinthine barrier are present in the affected side in patients with vestibular schwannoma. Furthermore, we found, although weak, positive correlation between post-contrast cochlear signal intensity on 3D-FLAIR images and the degree of hearing impairment. These results suggest that alteration of perilymph composition might be responsible for inner ear disorders in patients with vestibular schwannoma and that increased permeability of the blood–labyrinthine barrier might be closely related to the degree of hearing loss. These results warrant a further study to clarify the relationship between 3D-FLAIR findings and prognosis of hearing preservation surgery.

**Conflict of interest statement** We declare that we have no conflict of interest.

## References


1. Silverstein H, Schuknecht HF (1966) Biochemical studies of inner ear fluid in man: changes in otosclerosis, Meniere's disease, and acoustic neuroma. Arch Otolaryngol 84:395–402
2. Silverstein H (1971) Inner ear fluid proteins in acoustic neuroma, Meniere's disease, and otosclerosis. Ann Otol Rhinol Laryngol 80:27–35
3. Silverstein H (1973) Labyrinthine tap as a diagnostic test for acoustic neuroma. Otolaryngol Clin North Am 6:229–244
4. Silverstein H, Naufal P, Belal A (1973) Causes of elevated perilymph protein concentrations. Laryngoscope 83:476–487
5. Melhem ER, Jara H, Eustace S (1997) Fluid-attenuated inversion recovery MR imaging: identification of protein concentration threshold for CSF hyperintensity. AJR Am J Roentgenol 169:859–862
6. Mishra AM, Reddy SJ, Husain M, Behari S, Husain N, Prasad KN, Kumar S, Gupta RK (2006) Comparison of the magnetization transfer ratio and fluid-attenuated inversion recovery imaging signal intensity in differentiation of various cystic intracranial mass lesions and its correlation with biological parameters. J Magn Reson Imaging 24:52–56
7. Naganawa S, Koshikawa T, Nakamura T, Kawai H, Fukatsu H, Ishigaki T, Komada T, Maruyama K, Takizawa O (2004) Comparison of flow artifacts between 2D-FLAIR and 3D-FLAIR sequences at 3T. Eur Radiol 14:1901–1908
8. Sugiura M, Naganawa S, Sato E, Nakashima T (2006) Visualization of a high protein concentration in the cochlea of a patient with a large endolymphatic duct and sac, using three-dimensional fluid-attenuated inversion recovery magnetic resonance imaging. J Laryngol Otol 120:1084–1086
9. Sugiura M, Naganawa S, Teranishi M, Sato E, Kojima S, Nakashima T (2006) Inner ear hemorrhage in systemic lupus erythematosus. Laryngoscope 116:826–828
10. Otake H, Sugiura M, Naganawa S, Nakashima T (2006) 3D-FLAIR magnetic resonance imaging in the evaluation of mumps deafness. Int J Pediatr Otorhinolaryngol 70:2115–2117
11. Sugiura M, Naganawa S, Teranishi M, Nakashima T (2006) Three-dimensional fluid-attenuated inversion recovery magnetic resonance imaging findings in patients with sudden sensorineural hearing loss. Laryngoscope 116:1451–1454
12. Sone M, Mizuno T, Sugiura M, Naganawa S, Nakashima T (2007) Three-dimensional fluid-attenuated inversion recovery magnetic resonance imaging investigation of inner ear disturbances in cases of middle ear cholesteatoma with labyrinthine fistula. Otol Neurotol 28:1029–1033
13. Sugiura M, Naganawa S, Sone M, Yoshida T, Nakashima T (2008) Three-dimensional fluid attenuated inversion recovery magnetic resonance imaging findings in a patient with cochlear otosclerosis. Auris Nasus Larynx 35:269–272
14. Committee on Hearing and Equilibrium, American Academy of Otolaryngology-Head and Neck Surgery (1995) Committee on hearing and equilibrium guidelines for the evaluation of hearing preservation in acoustic neuroma (vestibular schwannoma). Otolaryngol Head Neck Surg 113:179–180
15. Eckermeier L, Pirsig W, Mueller D (1979) Histopathology of 30 non-operated acoustic schwannomas. Arch otorhinolaryngol 222:1–9
16. O'Connor AF, France MW, Morrison AW (1981) Perilymph total protein levels associated with cerebellopontine angle lesions. Am J Otol 2:193–195
17. Thomsen J, Saxtrup O, Tos M (1982) Quantitated determination of proteins in perilymph in patients with acoustic neuroma. ORL J Otorhinolaryngol Relat Spec 44:61–65
18. Naganawa S, Komada T, Fukatsu H, Ishigaki T, Takizawa O (2006) Observation of contrast enhancement in the cochlear fluid space of healthy subjects using a 3D-FLAIR sequence at 3 Tesla. Eur Radiol 16:733–737
19. Mathews VP, Caldemeyer KS, Lowe MJ, Greenspan SL, Weber DM, Ulmer JL (1999) Brain: gadolinium-enhanced fast fluid-attenuated inversion-recovery MR imaging. Radiology 211:257–263

20. Jackson EF, Hayman LA (2000) Meningeal enhancement on fast FLAIR images. Radiology 215:922–924
21. Kastenbauer S, Klein M, Koedel U, Pfister HW (2001) Reactive nitrogen species contribute to blood–labyrinth barrier disruption in suppurative labyrinthitis complicating experimental pneumococcal meningitis in the rat. Brain res 904:208–217
22. Nakashima T, Naganawa S, Sone M, Tominaga M, Hayashi H, Yamamoto H, Liu X, Nuttall AL (2003) Disorders of cochlear blood flow. Brain Res Brain Res Rev 43:17–28
23. Naganawa S, Sugiura M, Kawamura M, Fukatsu H, Nakashima T, Maruyama K (2006) Prompt contrast enhancement of cerebrospinal fluid space in the fundus of the internal auditory canal: observations in patients with meningeal diseases on 3D-FLAIR images at 3 Tesla. Magn Reson Med Sci 5:151–155
24. O'Connor AF, Luxon LM, Shortman RC, Thompson EJ, Morrison AW (1982) Electrophoretic separation and identification of perilymph proteins in cases of acoustic neuroma. Acta Otolaryngol 93:195–200
25. Palva T, Raunio V (1982) Cerebrospinal fluid and acoustic neuroma specific proteins in perilymph. Acta Otolaryngol 93:201–203
26. Rasmussen N, Bendtzen K, Thomsen J, Tos M (1983) Specific cellular immunity in acoustic neuroma patients. Otolaryngol Head Neck Surg 91:532–536
27. Rasmussen N, Bendtzen K, Thomsen J, Tos M (1984) Antigenicity and protein content of perilymph in acoustic neuroma patients. Acta Otolaryngol 97:502–508
28. Yoshida T, Sugiura M, Naganawa S, Teranishi M, Nakata S, Nakashima T (2008) Three-dimensional fluid-attenuated inversion recovery magnetic resonance imaging findings and prognosis in sudden sensorineural hearing loss. Laryngoscope 118:1433–1437
29. Gussen R (1976) Sudden deafness of vascular origin: a human temporal bone study. Ann Otol Rhinol Laryngol 85:94–100
30. Fitzgerald DC, Mark AS (1999) Viral cochleitis with gadolinium enhancement of the cochlea on magnetic resonance imaging scan. Otolaryngol Head Neck Surg 121:130–132
31. Barker GJ (1998) 3D fast FLAIR: a CSF-nulled 3D fast spin-echo pulse sequence. Magn Reson Imaging 16:715–720
32. Naganawa S, Kawai H, Fukatsu H, Ishigaki T, Komada T, Maruyama K, Takizawa O (2004) High-speed imaging at 3 Tesla: a technical and clinical review with an emphasis on whole-brain 3D imaging. Magn Reson Med Sci 3:177–187
33. Haacke EM, Frahm J (1991) A guide to understanding key aspects of fast gradient-echo imaging. J Magn Reson Imaging 1:621–624
34. Somers T, Casselman J, de Ceulaer G, Govaerts P, Offeciers E (2001) Prognostic value of magnetic resonance imaging findings in hearing preservation surgery for vestibular schwannoma. Otol Neurotol 22:87–94
35. Naganawa S, Satake H, Kawamura M, Fukatsu H, Sone M, Nakashima T (2008) Separate visualization of endolymphatic space, perilymphatic space and bone by a single pulse sequence; 3D-inversion recovery imaging utilizing real reconstruction after intratympanic Gd-DTPA administration at 3 Tesla. Eur Radiol 18:920–924
36. Naganawa S, Satake H, Iwano S, Fukatsu H, Sone M, Nakashima T (2008) Imaging endolymphatic hydrops at 3 Tesla using 3D-FLAIR with intratympanic Gd-DTPA administration. Magn Reson Med Sci 7:85–91
37. Naganawa S, Koshikawa T, Fukatsu H, Ishigaki T, Fukuta T (2001) MR cisternography of the cerebellopontine angle: comparison of three-dimensional fast asymmetrical spin-echo and three-dimensional constructive interference in the steady-state sequences. AJNR Am J Neuroradiol 22:1179–1185
38. Bhadelia RA, Tedesco KL, Hwang S, Erbay SH, Lee PH, Shao W, Heilman C (2008) Increased cochlear fluid-attenuated inversion recovery signal in patients with vestibular schwannoma. AJNR Am J Neuroradiol 29:720–723

International Journal of Pediatric Otorhinolaryngology 73 (2009) 1003–1005

Contents lists available at ScienceDirect

International Journal of Pediatric Otorhinolaryngology

journal homepage: www.elsevier.com/locate/ijporl

Case report

# Intratympanic membrane congenital cholesteatoma

Tadao Yoshida [a,*], Michihiko Sone [a], Terukazu Mizuno [b], Tsutomu Nakashima [a]

[a] Department of Otorhinolaryngology, Nagoya University Graduate School of Medicine, Nagoya, Japan
[b] Department of Otorhinolaryngology, Komaki City Hospital, 1-20 Jobushi, Komaki City, Aichi 485-8520, Japan

ARTICLE INFO

*Article history:*
Received 17 February 2009
Accepted 11 March 2009
Available online 16 April 2009

*Keywords:*
Intratympanic cholesteatoma
Congenital cholesteatoma

ABSTRACT

We present two, different-sized, intratympanic membrane congenital cholesteatomas. Congenital cholesteatoma within the tympanic membrane is extremely rare. One of our cases was a small pearl centered on the umbo and the other involved the whole of the tympanic membrane. In both cases the cholesteatomas involved only the outer epidermic layer of the tympanic membrane without extension into the fibrous layer. The intratympanic membrane cholesteatomas may eventually violate the middle ear space. We believe that early diagnosis and removal of intratympanic membrane cholesteatomas is necessary to avoid complications in the middle ear space.



## 1. Introduction

Congenital cholesteatoma within the tympanic membrane (TM) is very rare, with less than 20 cases of intratympanic membrane cholesteatoma without previous trauma or surgery to the ear reported in the literature to date [1]. Early diagnosis and treatment of cholesteatoma is essential because the lesion can advance just like any other cholesteatoma. We present two, different-sized, congenital cholesteatomas of the TM; one that was centered on the umbo and one that involved the whole of the TM.

## 2. Case reports

### 2.1. Case 1

A 3-year-old girl was noted by her local otolaryngologist to have a pearly white mass on the right tympanic membrane when she presented with an upper respiratory tract infection and was referred to our department for further investigation. Otomicroscopic examination revealed a normal left tympanic membrane and canal. However, on the right there was a small cholesteatoma pearl centered on the umbo (Fig. 1). The patient did not have any history of otitis media, otorrhea, ear trauma or otologic surgery. A pure tone audiogram revealed a 15-dB conductive hearing loss on the right side (for 500 and 1 kHz frequencies) compared to the left side. There was no other history of congenital abnormalities. A high resolution computed tomography (CT) scan of the temporal bones showed a soft round tissue mass, 2.5 mm in diameter, located on the external surface of the right TM and did not reveal any middle ear extension (Fig. 2). An endaural approach was performed and the cholesteatoma pearl was easily enucleated from the TM. The pearl-shaped cholesteatoma involved only the outer epidermic layer of the TM without extension into the fibrous layer. After removal, myringoplasty was not necessary since the integrity of the fibrous layer of the TM had not been violated. Histopathology confirmed a cholesteatoma.

### 2.2. Case 2

A 3-year-old girl was referred to our department by her otolaryngologist who noted a white mass on the right external auditory canal. Otomicroscopic examination revealed a white mass over the whole of the right TM (Fig. 3). There was no history of otitis media, otorrhea, ear trauma, otologic surgery or vertigo. Examination revealed a normal left TM and external auditory canal. Obtaining an audiogram was not possible and thus the auditory evoked brainstem response (ABR) threshold was estimated to be 60-dB SPL. A CT scan of temporal bone showed a soft tissue mass occupying the external ear canal, and the middle ear cavity (Fig. 4). We suspected that the mass had invaded the middle ear space and made contact with the ossicles. Surgery was performed by an endaural approach. After reduction in the size of the cholesteatoma, the lesion could be removed from the intact fibrous layer of the TM. There was no invasion into the middle ear space. Histopathology confirmed a cholesteatoma. At a 1-year follow-up, otomicroscopy revealed that the

* Corresponding author at: Department of Otorhinolaryngology, Nagoya University Graduate School of Medicine, 65 Tsurumai-cho, Showa-ku, Nagoya 466-8550, Japan. Tel.: +81 52 744 2323/568 76 4131; fax: +81 52 744 2325/568 76 4145.
*E-mail address:* tadaoy@med.nagoya-u.ac.jp (T. Yoshida).

0165-5876/$ – see front matter © 2009 Elsevier Ireland Ltd. All rights reserved.
doi:10.1016/j.ijporl.2009.03.005